Author Manuscript

Ketotifen Modulates Mast Cell Chemotaxis to Kit-Ligand, but Does Not Impact Mast Cell Numbers, Degranulation, or Tumor Behavior in Neurofibromas of *Nf1-* Deficient Mice

Ciersten A. Burks[1], **Steven D. Rhodes**[1], **Waylan K. Bessler**[1], **Shi Chen**[1], **Abbi Smith**[1], **Jeffrey R. Gehlhausen**[1], **Eric T. Hawley**[1], **Li Jiang**[1], **Xiaohong Li**[1], **Jin Yuan**[1], **Qingbo Lu**[1], **Max Jacobsen**[2], **George Sandusky**[2], **David R. Jones**[3], **D. Wade Clapp**[1,4,5,#,¶], **Jaishri Blakeley**[6,7,#,¶]

[1]Herman B. Wells Center for Pediatric Research, Indiana University School of Medicine

[2]Department of Pathology and Laboratory Medicine, Indiana University School of Medicine

[3]Department of Medicine, Division of Clinical Pharmacology, Indiana University School of Medicine

[4]Department of Microbiology and Immunology, Johns Hopkins University School of Medicine, Baltimore, MD, USA

[5]Department of Biochemistry and Molecular Biology, Johns Hopkins University School of Medicine, Baltimore, MD, USA

[6]Department of Neurology, Johns Hopkins University School of Medicine, Baltimore, MD, USA

[7]Department of Oncology, Johns Hopkins University School of Medicine, Baltimore, MD, USA

Abstract

Neurofibromatosis Type 1 (NF1) is one of the most common genetic tumor predisposition syndromes in humans. Mutant *NF1* results in dysregulated RAS allowing neoplasms throughout the neuroaxis. Plexiform neurofibromas (pNFs) afflict up to 50% of patients with NF1. They are complex tumors of the peripheral nerve that cause major morbidity via nerve dysregulation and mortality via conversion to malignant sarcoma. Genetically engineered mouse models (GEMMs) of NF1 provide valuable insights for the identification of therapies that have utility in people with pNF. Preclinical studies in GEMMs implicate mast cells and the c-Kit/Kit ligand pathway in pNF tumorigenesis. Kit ligand is a potent chemokine secreted by tumorigenic, *Nf1-deficient* Schwann cells. Ketotifen is an FDA-approved drug for the treatment of allergic conjunctivitis and asthma that promotes mast cell stabilization and has been used in prior case studies to treat or prevent pNFs. This study investigated the effect of ketotifen on mast cell infiltration and degranulation in

the presence and absence of Kit ligand provocation and the effect of ketotifen on shrinking or preventing pNF formation in the *Nf1^{flox/flox}*;*PostnCre+* GEMM. Ketotifen decreased mast cell infiltration in response to exogenous Kit ligand administration, but did not affect mast cell degranulation. Importantly, ketotifen did not reduce mast cells numbers or activity in pNF and did not prevent pNF formation or decrease the volume of established pNF despite administration of pharmacologically active doses. These findings suggest ketotifen has limited use as monotherapy to prevent or reduce pNF burden in the setting of *Nf1* mutations.

Keywords

neurofibromatosis type 1; NF1; plexiform neurofibroma; ketotifen

INTRODUCTION

Neurofibromatosis type 1 (NF1) is an autosomal dominant cancer predisposition syndrome with a prevalence of 1 in 2,600 to 3,000 across all populations of the world (1,2). NF1 syndrome is caused by mutations of the *NF1* tumor suppressor gene encoding the protein neurofibromin, which functions as a GTPase activating protein for p21 Ras. Loss of both alleles of *NF1* in the tumor-initiating cells results in constitutive activation of Ras and its downstream effectors, ultimately leading to tumor formation. *Nf1* is the murine homologue of the human *NF1*. It is highly conserved both structurally and in biochemical and cellular function across species.

Plexiform neurofibromas (pNFs) are a hallmark manifestation of NF1. These multicellular tumors arise from peripheral nerves and afflict approximately 50% of patients with NF1 (3,4). pNFs frequently result in debilitating disfigurement, organ dysfunction (3–6), neurologic dysfunction (7,8), chronic pain (9), and have a propensity for malignant conversion (1,2,10). Further, pNFs are resistant to many targeted and standard chemotherapies and, due to their intercalation within nerves, cannot be completely removed without sacrificing functioning nerve (11–14). pNF consist of a mixture of Schwann cells, fibroblasts, endothelial cells, and inflammatory mast cells (15–19). *NF1* (*Nf1*) deficient Schwann cells are the established tumorigenic cell of origin for pNF formation (16,19). However, detailed serial dissection studies show that mast cells are the first microenvironment cell drawn to the tumorigenic nidus (15,17,18,20). Further, genetic and adoptive transfer studies in genetically engineered mice show that tumorigenic initiation is dependent on c-Kit/Kit ligand, the key chemokine and growth factor for all aspects of mast cell development and function (15,17,18). *Nf1*-deficient Schwann cells secrete pathologically elevated levels of Kit ligand (17,20,21). Thus, through *Nf1*-deficient Schwann cell-mediated Kit ligand secretion, mast cells are recruited to the site of the tumorigenic nidus where they release multiple cytokines and matrix metalloproteinases that promote neoangiogenesis, fibroblast recruitment, and collagen deposition (15,17,18,20–23).

Our group has shown that targeting c-Kit/Kit ligand with imatinib mesylate leads to significant reduction in pNF size in preclinical models of pNF and that imatinib had similar activity in humans; particularly young children with NF1 associated pNF (18,22–24).

Ketotifen is a mast cell stabilizer and noncompetitive H1-antihistamine approved for the treatment of asthma and allergic conjunctivitis that is well tolerated and inexpensive. Small, non-randomized human trials dating to the 1980s have evaluated ketotifen in people with NF1 based on the rationale of mast cell stabilization (25–27). These studies reported subjective activity of ketotifen with the largest study being a combination of a controlled study and an observations study of 52 patients given 2–4 mg ketotifen per day for up to 78 months and the endpoint being patient reports of benefit based on recall (26). No formal measurements of tumor growth or tumor reduction were obtained in these studies (25–27). Although the data reported are limited in nature, they suggest that pharmacologic mast cell stabilization with ketotifen may have therapeutic benefit for people with NF1 associated neurofibromas. Given the safety profile of ketotifen in patients treated for asthma, validation of its efficacy in tumor reduction or prevention is of great value to the NF1 patient community.

A limitation in the use of effective therapies for many pediatric orphan disease cancers is the availability of adequate patient populations to formally test drug efficacy. The development of genetically engineered mouse models (GEMM) that closely recapitulate the developmental pathogenesis of human tumors provides an opportunity to test therapies in preclinical models in a way that was not available previously (28). There are now multiple instances where preclinical studies in *Nf1* GEMMs have led to the identification of drugs that are active in patients (24,28,29). Importantly, studying GEMMs provides the opportunity to critically examine the mechanism of action of small molecules and ensure adequate pharmacokinetics (PK) are achieved before assessing efficacy endpoints.

The aim of this study was to investigate the efficacy and mechanism of action of ketotifen in the treatment of NF1-associated pNF. The primary objective was to determine whether ketotifen monotherapy is sufficient to reduce or prevent pNF formation in a highly validated GEMM of pN (18,24). In addition, given ketotifen's hypothesized role in ameliorating or preventing pNF formation via stabilization of the mast cell, we conducted a series of experiments to test whether ketotifen effectively prevents mast cell recruitment and degranulation in response to Kit ligand stimulation in this model (30,31).

METHODS AND MATERIALS

Study approval

The animal protocol #10932 was approved by the Institutional Animal Care and Use Committee of Indiana University School of Medicine and all studies were carried out accordingly.

Animals, kit ligand, and ketotifen administration

The *Nf1^flox/flox^;PostnCre+* mice were developed and bred by the Clapp Laboratory utilizing tools reported previously (18). Tumor formation is driven by the early embryonic conditional deletion of *Nf1* in Schwann cell progenitors via the Periostin (Postn) promoter and Cre recombinase enzyme (32,33). *Nf1^flox/flox^;PostnCre+* mice develop neurofibromas with complete penetrance that are measureable at roughly four months of age. Ketotifen fumarate

was purchased from Sigma-Aldrich. In the prevention and intervention therapeutic studies, ketotifen 1 mg/mL was prepared in ddH$_2$O and administered via oral gavage at 10 mg/kg once daily seven days/week. Vehicle-treated *Nf1$^{flox/flox}$*;*PostnCre+* mice were administered 0.1 mg/day water via oral gavage. The control and treatment cohorts of mice were weighed daily to determine the safety and tolerability of ketotifen throughout the duration of the treatment period. Following 12 weeks of treatment, mice in the prevention study (water/ vehicle-treated n = 6, ketotifen-treated n = 6) were sacrificed at four months of age (Figure 1A) and mice in the tumor treatment study (water/vehicle-treated n = 15, ketotifen-treated n = 14) were sacrificed at seven months of age (Figure 2A).

To determine if ketotifen had an *in vivo* effect on mast cell infiltration and degranulation, four-month old *Nf1$^{+/-}$* mice were administered subcutaneous Kit Ligand as previously described (34). Briefly, *Nf1$^{+/-}$* mice were pre-treated with 10 mg/kg/d of ketotifen or 10 mg/kg/d of water administered via oral gavage from days zero-seven. On day seven, a mid-dorsum micro-osmotic pump was implanted and the mice received a continuous infusion of 20 μg/kg/d Kit ligand or control PBS, as previously described (34). Oral ketotifen treatment or water was continued throughout days 7–14. On day 14, skin biopsies near the site of the micro-osmotic pump were harvested and stained with toluidine blue for quantification of mast cell infiltration and degranulation (Figure 3A).

Quantification of ketotifen

Ketotifen was quantified in plasma and nerve tissue samples from ketotifen-treated *Nf1$^{flox/flox}$*;*PostnCre+* mice (n = 3) by HPLC-MS/MS (Agilent 1200 HPLC and ABI 3200 MS/MS) (35). The animals received a single dose of 10 mg/kg ketotifen. Plasma samples were obtained at one, two, four, eight and 24 hours post-ketotifen dose. Tissue samples from sciatic, brachial and trigeminal nerve were obtained at four and 24 hours post-ketotifen dose. A method to quantify ketotifen in plasma was developed using temazepam as the internal standard, liquid- liquid extraction, and HPLC-MS/MS. Variability was minimized in the method by using methyl tert-butyl ether instead of ethyl acetate, dichloroethane, or hexane:ethyl acetate as the solvent and polypropylene tubes instead of glass tubes. The mobile phase uses formic acid instead of ammonium acetate. The lower limit of quantification is one ng/mL using 20 μL of plasma. A set of eight standards were run for each batch of plasma or tissue samples.

Nerve/Tumor volume quantitation

Following microscopic dissection of the spinal proximal nerves, nerve volume was measured by calipers and calculated by the established approximation for the volume of a spheroid, $0.52 \times (\text{width})^2 \times \text{length}$. Four proximal nerves per mouse were measured as previously described (18).

Histology and immunohistochemistry

To examine tumor morphology and the extent of mast cell infiltration, spinal proximal nerves and peripheral nerves were dissected from 4–7 month old *Nf1$^{flox/flox}$*;*PostnCre+* mice, fixed in 10% formalin, processed through graded alcohols, xylenes and molten paraffin, embedded in paraffin, and subsequently sectioned and stained with hematoxylin

and eosin (H&E), toluidine blue (to identify mast cells) and Masson's trichrome stain for collagen and tumor quantification.

DATA ANALYSIS

Statistical methods

GraphPad Prism 5.0 and 6.0 was used to perform all statistical analyses. Comparison of the means for nerve root volume, tumor number, KI-67 proliferation index, number of infiltrating mast cells, number of degranulating mast cells, and percentage of degranulating mast cells was performed using the two-tailed, unpaired Student's t test and one-way analysis of variance (ANOVA) with Tukey's test post-hoc analysis. P-values of < 0.05 were considered statistically significant for all tests.

Pharmacokinetic data analysis

Pharmacokinetic parameters for ketotifen including area under the curve (AUC) and $t\frac{1}{2}$ were estimated using noncompartmental methods with add-ins in Excel®. The maximum plasma concentration (C_{max}) was obtained from the data. The AUC from zero to infinity ($AUC_{0-\infty}$) was estimated from the AUC_{0-t} (time zero to the last quantifiable concentration C_{last}) and the AUC from C_{last} to infinity, C_{last}/k_{el}, where k_{el} is the rate constant of elimination.

IMAGE ANALYSIS

Toluidine blue is a histological stain specific for mast cells. To avoid user bias, toluidine blue-stained histological images were scanned in on a Leica ScanScope and HALO software v2.0.1038 was used for image analysis in scoring total and degranulating mast cells. The Cytonuclear algorithm was used to quantify mast cells in the skin. Using a toluidine blue stain, the Cytonuclear algorithm uses a dark blue positive stain (0.992, 0.65558, 0.219 RGB OD) against a light blue (1.176, 1.260, 0.621 RGB OD) background. The intensity threshold was narrowed from the standard immunostain algorithm of 0.112, 0.287, 0.445 (weak, moderate, strong) to 0.300, 0.340, 0.355 (weak, moderate, strong). Two sets of analyses were run, only altering the minimum nuclear roundness parameter between the two analyses. The first run is a minimum nuclear roundness of 0.0 to include all mast cells. Then the minimum nuclear roundness was raised to 0.6 and reanalyzed to quantify mast cells that were not degranulating. The difference between the total and the non-degranulating population was determined to be the total degranulating population.

RESULTS

Ketotifen does not prevent neurofibroma genesis in *Nf1^flox/flox^;PostnCre+* mice

A major goal for genetic tumor predisposition syndromes like NF1 is the prevention of tumor formation. Given the high therapeutic index of ketotifen and the mechanistic link between mast cells, c-Kit/Kit ligand, and pNF formation we hypothesized ketotifen may prevent or alter the latency of tumorigenesis. *Nf1^flox/flox^;PostnCre+* mice begin to acquire Schwann cell hyperplasia at approximately 4–6 weeks of age prior to the formation of multiple pNFs. To test our hypothesis, we employed the experimental design outlined in

Figure 1A. *Nf1^flox/flox;PostnCre+* mice (n = 6) were treated with 10 mg/kg of ketotifen from 5–6 weeks post-natal, prior to the genesis of pNFs, until four months of age when they were sacrificed. At necropsy, there was no difference in nerve hyperplasia between the treatment and water/vehicle-treated *Nf1^flox/flox;PostnCre+* mice (Figure 1B, ns). Further, microscopic evaluation revealed that ketotifen treatment did not reduce the number of mast cells infiltrating nerve tissue (Figure 1C and 1D, ns) nor did it reduce the percentage of degranulating mast cells (Figure 1C and 1E, ns).

Ketotifen does not reduce proximal nerve root volume or tumor number in *Nf1^flox/flox;PostnCre+* mice

Nf1^flox/flox;PostnCre+ mice uniformly acquire multiple pNFs by four months of age. To model the treatment of human pNF-harboring NF1, we followed the experimental design outlined in Figure 2A. *Nf1^flox/flox;PostnCre+* mice were treated from four to seven months of age to assess the impact of ketotifen on established tumors. There was no statistical difference in proximal nerve root volume (Figure 2B, ns) or tumor number (Figure 2C, ns) between ketotifen (n = 14) and water/vehicle-treated (n = 14) *Nf1^flox/flox;PostnCre+* groups. Tumor number ranged from 0–22 in water/vehicle-treated *Nf1^flox/flox;PostnCre+* mice and 0–20 in the ketotifen-treated *Nf1^flox/flox;PostnCre+* mice at seven months. Both ketotifen and water/vehicle-treated *Nf1^flox/flox;PostnCre+* mice demonstrated a significantly greater proximal nerve root volume compared to historic age, sex and strain-related *Nf1^flox/flox;PostnCre-* WT mice that did not develop tumors (Figure 2B and 2C). Further, microscopic evidence revealed no significant difference in the quantity of mast cells infiltrating peripheral nerve tumor tissue in ketotifen-treated mice compared to mice receiving water vehicle (Figure 2D and 2E). Finally, ketotifen treatment failed to reduce the percentage of degranulating mast cells when compared to water/vehicle-treated mice (Figure 2D and 2F).

Effect of Kit ligand and ketotifen, alone or in combination, on mast cell infiltration and degranulation in skin

Prior work in genetically engineered mice established that the c-Kit/Kit ligand pathway is central in pNF tumor initiation (18,20–22). This work has been replicated using a variety of Cre drivers with similar results (unpublished data, WC, SC and WB). Given that c-Kit impacts the development, migration, proliferation, and degranulation of mast cells *in vitro* and *in vivo* we assessed the impact of ketotifen on preventing mast cell infiltration and degranulation following a Kit ligand infusion using an established protocol (17,20,34–37). Consistent with the previous studies, Kit ligand infusion revealed a statistically significant increase in mast cell infiltrate (Figure 3C and 3D, $P < 0.0001$). Kit ligand infusion had no impact on the percentage of degranulating mast cells relative to PBS infusion (Figure 3E, $P > 0.05$). We then evaluated the effect of ketotifen on mast cell infiltration and degranulation in the presence and absence of Kit ligand infusion. In mice receiving Kit ligand infusion, ketotifen treatment decreased the number of infiltrating mast cells when compared with water treatment (Figure 3D, $P < 0.0001$). However, ketotifen treatment failed to induce a significant decrease in the percentage of degranulating mast cells (Figure 3E, ns) in mice receiving the Kit ligand infusion. These results indicate that ketotifen is not effective in inhibiting all Kit ligand-mediated mast cell functions in *Nf1^{+/−}* mice, including the

inhibition of Kit-mediated mast cell degranulation, at least at pharmacologic concentrations utilized in these experiments.

Pharmacokinetics of ketotifen in *Nf1*-deficient mice

After a single dose of ketotifen at 10 mg/kg in $Nf1^{flox/flox}$;*PostnCre+* tumor-bearing mice, the maximum plasma concentration was 40 ng/mL, $AUC_{0-\infty}$ 119 ng/mL·h, and $t_{1/2}$ 29.9 hours (Figure 4A, n = 3 at each time point). These data are slightly greater than the values estimated in humans (35).The concentration of ketotifen in sciatic, brachial, and trigeminal nerve tissue was also measured at four and 24 hours after a single dose of ketotifen 10 mg/kg (n = 6) to confirm that the drug reached the site of tumor initiation. At four hours, the mean concentration of ketotifen in all nerves measured was 14.56 ng/g of nerve tissue (Figure 4B), while at 24 hours the concentration of ketotifen in all nerve tissue samples was below the level of quantification (data not shown).

Safety and Tolerability

The tolerability of ketotifen in $Nf1^{flox/flox}$;*PostnCre+* mice was measured with daily weights throughout the 12-week treatment period of established tumors. There was no significant difference between the vehicle-treated (n = 15) versus ketotifen-treated (n = 14) cohorts in weight.

DISCUSSION

Neurofibromas are the hallmark tumor of the NF1 syndrome. pNFs start very early in life (many are thought to be congenital) and grow rapidly through early childhood resulting in nerve sheath tumors that cause pain, neurologic dysfunction, disfigurement and roughly 10% of the time convert to the highly aggressive sarcoma, malignant peripheral nerve sheath tumor (1–3,5–10). Given their prevalence and the lack of effective therapies to prevent or reduce the impact of these tumors, major efforts from multiple laboratories are being pursued to reduce the size and morbidity associated with these tumors (28). The drugs being utilized currently in preclinical models and in clinical trials are overwhelmingly small-molecule targeted therapies (28). While some of these therapies show significant promise, there are common, on-target adverse effects that limit their use. For example, though overall largely well-tolerated, both imatinib mesylate and selumetinib caused a variety of symptoms including gastrointestinal reactions, edema, muscle cramps, fatigue and acneiform rash that limit their long term tolerability (24,29,38,39). Further, the cost of these novel drugs could be substantial and long-term safety is unknown. Thus, the hypothesis that a drug like ketotifen which has a high therapeutic index, is low cost and shown to be safe for long term use with a hint of clinical activity in prior studies provided the rationale for formal testing in a preclinical model of NF1 pNF.

Specifically, the clinical studies using ketotifen in patients with NF1 conducted in the 1980s and 1990s preceded the current understanding of the cellular and molecular pathways underlying the genesis of pNFs and hence, mechanism was not examined. In addition, the prior clinical studies with ketotifen used efficacy evaluations that are outside of the recommended endpoints for pNF in the modern era (40–42). Hence, the community is left

with reports of symptomatic improvement with non-validated measures and an interesting hypothesis about the biologic effect of ketotifen on pNF without evidence of mechanism. Given this conundrum, we conducted a formal preclinical study to evaluate the PK, mechanism of action and efficacy of ketotifen in a manner similar to preclinical studies pursued with imatinib mesylate and selumetinib prior to clinical use (17,29).

We found that maximum drug concentrations in both plasma (40 ng/mL) and target tissue sites (14.56 ng/g) including sciatic, brachial and trigeminal nerve with 10 mg/kg ketotifen were significantly greater than the levels achieved in published human plasma PK studies (2 mg/kg, C_{max} 449 pg/mL) even after adjusting for the dose administered, and had a $t_{1/2}$ (29.9 hrs) significantly longer than that previously reported in the plasma of human patients (4.4 hrs) (Figure 4A–B) (35). There is no published human tissue PK for ketotifen. Thus, we conclude that both systemic and tissue-specific drug concentrations were sufficient to achieve biologic effects.

Regrettably, we found ketotifen did not alter tumor burden when treatment was started after tumor formation in *Nf1flox/flox;PostnCre+* mice (Figure 2B and 2C). This is consistent with case series reporting that ketotifen had no effect on established tumors in adults with NF1 (43).

NF1 is characterized by rapid growth of pNFs beginning in infancy and throughout childhood (8,44,45). Therefore, the identification of a drug that prevents early tumor initiation and progression would have great therapeutic value. Based on prior unpublished studies in our laboratory, we have demonstrated that *Nf1flox/flox;PostnCre+* mice acquire Schwann cell hyperplasia at approximately four to six weeks of age and acquire multiple pNFs by four months of age (S.D. Rhodes, unpublished data). In order to model a pNF prevention therapeutic strategy in mice, *Nf1flox/flox;PostnCre+* mice were treated from five or six weeks of age until four months of age with ketotifen (Figure 1A). Again, at the conclusion of the 12-week treatment period, there was no difference in proximal nerve root volume or mast cell infiltration between vehicle and ketotifen-treated cohorts of *Nf1flox/flox;PostnCre+* mice (Figure 1B–E).

The interaction between Schwann cells, the established tumorigenic cell in pNF, and the tumor microenvironment has been demonstrated in multiple GEMMs (17,18,20,21). Kit ligand is one key mediator of tumor initiation and progression (17,20–23). The exact mechanism by which c-Kit+ positive cells, such as mast cells, function to induce tumor development in response to Kit stimulation remains incompletely understood. However, prior work by our laboratory established that Kit ligand secreted at pathologically elevated levels by *Nf1*-deficient Schwann cells promotes multiple aspects of mast cell development and function including migration, proliferation, survival, degranulation, and secretion of *de novo* synthesized cytokines independent of pre-stored granules (17,20–23). The pre-stored and *de novo* synthesized biologically active products released by mast cells (matrix metalloproteinases, angiogenin, βFGF, MCP-1, VEGF and IL-8) play essential roles in tumor biology by promoting angiogenesis, monocyte recruitment, and tissue remodeling (37,46). The present studies demonstrate that ketotifen fails to exert a meaningful impact *in vivo* on mast cell infiltration, degranulation, or on tumor development in both established

tumors and in a prevention model. Interestingly, a recent genetic study demonstrated that significant declines in Kit ligand and mast cell numbers in existing plexiform neurofibromas have minimal impact on tumor growth (47). It is possible that other infiltrating immune lineages, including macrophages, which are abundant constituents of the plexiform neurofibroma microenvironment may play a critical role in tumor progression. This concept warrants further investigation. Though we cannot exclude the potential of species-specific differences in pharmacologic activity, there has been high fidelity of this preclinical model and subsequent clinical trials using other targeted therapeutics, including with the modulation of the c-Kit pathway (18,24,28). Collectively, our data suggests that ketotifen fails to modulate mast cell infiltration or degranulation in pNF and is insufficient as monotherapy for the treatment and prevention of these tumors.

ACKNOWLEDGEMENTS

Abbreviations key

NF1	Neurofibromatosis Type 1 (disease)
pNF	plexiform neurofibroma
Nf1	*Nf1* murine gene
GEMM	genetically engineered mouse model
NF1	*NF1* human gene
Postn	Periostin
HPLC MS/MS	High Performance Liquid Chromatograph Tandem Mass Spectrometry
N	number (i.e. of animals)
Mg	Milligram
Kg	Kilogram
Ng	Nanogram

| PBS | phosphate buffered saline |
AUC	area under the curve
$AUC_{0-\infty}$,	area under the curve from zero to infinity
RGB OD	Red Green Blue Optical Density
mL	Milliliter
H	Hour
G	Gram
Ns	not significant
P	p value
βFGF	beta fibroblast growth factor
MCP	monocyte chemoattractant protein
VEGF	vascular endothelial growth factor
IL	Interleukin
ddH2O	sterile ultra pure water
μg	Microgram
D	Day
μL	Microliter
$t^{1/2}$	half-life
WT	wild-type

References

1. Evans DG, Howard E, Giblin C, Clancy T, Spencer H, Huson SM, et al. Birth incidence and prevalence of tumor-prone syndromes: estimates from a UK family genetic register service. Am J Med Genet A 2010;152A(2):327–32 doi 10.1002/ajmg.a.33139. [PubMed: 20082463]

2. Uusitalo E, Leppavirta J, Koffert A, Suominen S, Vahtera J, Vahlberg T, et al. Incidence and mortality of neurofibromatosis: a total population study in Finland. J Invest Dermatol 2015;135(3):904–6 doi 10.1038/jid.2014.465. [PubMed: 25354145]

3. Huson SM, Harper PS, Compston DA. Von Recklinghausen neurofibromatosis. A clinical and population study in south-east Wales. Brain 1988;111 (Pt 6):1355–81. [PubMed: 3145091]

4. Plotkin SR, Bredella MA, Cai W, Kassarjian A, Harris GJ, Esparza S, et al. Quantitative assessment of whole-body tumor burden in adult patients with neurofibromatosis. PLoS One 2012;7(4):e35711 doi 10.1371/journal.pone.0035711. [PubMed: 22558206]

5. Avery RA, Dombi E, Hutcheson KA, Acosta MT, Baldwin AM, Madigan WP, et al. Visual outcomes in children with neurofibromatosis type 1 and orbitotemporal plexiform neurofibromas. Am J Ophthalmol 2013;155(6):1089–94 e1 doi 10.1016/j.ajo.2013.01.011. [PubMed: 23453281]

6. Calligaris L, Marchetti F, Ventura A. Intestinal plexiform neurofibromas. Dig Liver Dis 2008;40(7):578 doi 10.1016/j.dld.2007.12.013. [PubMed: 18294937]

7. Creange A, Zeller J, Rostaing-Rigattieri S, Brugieres P, Degos JD, Revuz J, et al. Neurological complications of neurofibromatosis type 1 in adulthood. Brain 1999;122 (Pt 3):473–81. [PubMed: 10094256]

8. Kim A, Gillespie A, Dombi E, Goodwin A, Goodspeed W, Fox E, et al. Characteristics of children enrolled in treatment trials for NF1-related plexiform neurofibromas. Neurology 2009;73(16):1273–9 doi 10.1212/WNL.0b013e3181bd1326. [PubMed: 19841379]

9. Wolters PL, Martin S, Merker VL, Tonsgard JH, Solomon SE, Baldwin A, et al. Patient-reported outcomes of pain and physical functioning in neurofibromatosis clinical trials. Neurology 2016;87(7 Suppl 1):S4–S12 doi 10.1212/WNL.0000000000002927.

10. Nguyen R, Jett K, Harris GJ, Cai W, Friedman JM, Mautner VF. Benign whole body tumor volume is a risk factor for malignant peripheral nerve sheath tumors in neurofibromatosis type 1. J Neurooncol 2014;116(2):307–13 doi 10.1007/s11060-013-1293-1. [PubMed: 24166582]

11. Canavese F, Krajbich JI. Resection of plexiform neurofibromas in children with neurofibromatosis type 1. J Pediatr Orthop 2011;31(3):303–11 doi 10.1097/BPO.0b013e31820cad77. [PubMed: 21415691]

12. Weiss B, Widemann BC, Wolters P, Dombi E, Vinks AA, Cantor A, et al. Sirolimus for non-progressive NF1-associated plexiform neurofibromas: an NF clinical trials consortium phase II study. Pediatr Blood Cancer 2014;61(6):982–6. [PubMed: 24851266]

13. Widemann BC, Babovic-Vuksanovic D, Dombi E, Wolters PL, Goldman S, Martin S, et al. Phase II trial of pirfenidone in children and young adults with neurofibromatosis type 1 and progressive plexiform neurofibromas. Pediatr Blood Cancer 2014;61(9):1598–602 doi 10.1002/pbc.25041. [PubMed: 24753394]

14. Widemann BC, Dombi E, Gillespie A, Wolters PL, Belasco J, Goldman S, et al. Phase 2 randomized, flexible crossover, double-blinded, placebo-controlled trial of the farnesyltransferase inhibitor tipifarnib in children and young adults with neurofibromatosis type 1 and progressive plexiform neurofibromas. Neuro Oncol 2014;16(5):707–18 doi 10.1093/neuonc/nou004. [PubMed: 24500418]

15. Hirota S, Nomura S, Asada H, Ito A, Morii E, Kitamura Y. Possible involvement of c-kit receptor and its ligand in increase of mast cells in neurofibroma tissues. Arch Pathol Lab Med 1993;117(10):996–9. [PubMed: 7692836]

16. Le LQ, Liu C, Shipman T, Chen Z, Suter U, Parada LF. Susceptible stages in Schwann cells for NF1-associated plexiform neurofibroma development. Cancer Res 2011;71(13):4686–95 doi 10.1158/0008-5472.CAN-10-4577. [PubMed: 21551250]

17. Yang FC, Ingram DA, Chen S, Hingtgen CM, Ratner N, Monk KR, et al. Neurofibromin-deficient Schwann cells secrete a potent migratory stimulus for Nf1+/− mast cells. J Clin Invest 2003;112(12):1851–61 doi 10.1172/JCI19195. [PubMed: 14679180]

18. Yang FC, Ingram DA, Chen S, Zhu Y, Yuan J, Li X, et al. Nf1-dependent tumors require a microenvironment containing Nf1+/−- and c-kit-dependent bone marrow. Cell 2008;135(3):437–48 doi 10.1016/j.cell.2008.08.041. [PubMed: 18984156]

19. Zhu Y, Ghosh P, Charnay P, Burns DK, Parada LF. Neurofibromas in NF1: Schwann cell origin and role of tumor environment. Science 2002;296(5569):920–2 doi 10.1126/science.1068452. [PubMed: 11988578]

20. Chen S, Burgin S, McDaniel A, Li X, Yuan J, Chen M, et al. Nf1−/− Schwann cell-conditioned medium modulates mast cell degranulation by c-Kit-mediated hyperactivation of phosphatidylinositol 3-kinase. Am J Pathol 2010;177(6):3125–32 doi 10.2353/ajpath.2010.100369. [PubMed: 21037083]

21. Ingram DA, Yang FC, Travers JB, Wenning MJ, Hiatt K, New S, et al. Genetic and biochemical evidence that haploinsufficiency of the Nf1 tumor suppressor gene modulates melanocyte and mast cell fates in vivo. J Exp Med 2000;191(1):181–8. [PubMed: 10620616]

22. Lasater EA, Bessler WK, Mead LE, Horn WE, Clapp DW, Conway SJ, et al. Nf1+/− mice have increased neointima formation via hyperactivation of a Gleevec sensitive molecular pathway. Hum Mol Genet 2008;17(15):2336–44 doi 10.1093/hmg/ddn134. [PubMed: 18442999]

23. Staser K, Yang FC, Clapp DW. Pathogenesis of plexiform neurofibroma: tumor-stromal/ hematopoietic interactions in tumor progression. Annu Rev Pathol 2012;7:469–95 doi 10.1146/ annurev-pathol-011811-132441. [PubMed: 22077553]

24. Robertson KA, Nalepa G, Yang FC, Bowers DC, Ho CY, Hutchins GD, et al. Imatinib mesylate for plexiform neurofibromas in patients with neurofibromatosis type 1: a phase 2 trial. Lancet Oncol 2012;13(12):1218–24 doi 10.1016/S1470-2045(12)70414-X. [PubMed: 23099009]

25. Riccardi VM. Mast-cell stabilization to decrease neurofibroma growth. Preliminary experience with ketotifen. Arch Dermatol 1987;123(8):1011–6. [PubMed: 3115189]

26. Riccardi VM. A controlled multiphase trial of ketotifen to minimize neurofibroma-associated pain and itching. Arch Dermatol 1993;129(5):577–81. [PubMed: 8481017]

27. Riccardi VM. Ketotifen suppression of NF1 neurofibroma growth over 30 years. Am J Med Genet A 2015;167(7):1570–7 doi 10.1002/ajmg.a.37045. [PubMed: 25974154]

28. Maertens O, McCurrach ME, Braun BS, De Raedt T, Epstein I, Huang TQ, et al. A Collaborative Model for Accelerating the Discovery and Translation of Cancer Therapies. Cancer Res 2017;77(21):5706–11 doi 10.1158/0008-5472.CAN-17-1789. [PubMed: 28993414]

29. Dombi E, Baldwin A, Marcus LJ, Fisher MJ, Weiss B, Kim A, et al. Activity of Selumetinib in Neurofibromatosis Type 1-Related Plexiform Neurofibromas. N Engl J Med 2016;375(26):2550– 60 doi 10.1056/NEJMoa1605943. [PubMed: 28029918]

30. Costa JJ, Demetri GD, Harrist TJ, Dvorak AM, Hayes DF, Merica EA, et al. Recombinant human stem cell factor (kit ligand) promotes human mast cell and melanocyte hyperplasia and functional activation in vivo. J Exp Med 1996;183(6):2681–6. [PubMed: 8676090]

31. Taylor AM, Galli SJ, Coleman JW. Stem-cell factor, the kit ligand, induces direct degranulation of rat peritoneal mast cells in vitro and in vivo: dependence of the in vitro effect on period of culture and comparisons of stem-cell factor with other mast cell-activating agents. Immunology 1995;86(3):427–33. [PubMed: 8550081]

32. Gehlhausen JR, Park SJ, Hickox AE, Shew M, Staser K, Rhodes SD, et al. A murine model of neurofibromatosis type 2 that accurately phenocopies human schwannoma formation. Hum Mol Genet 2015;24(1):1–8 doi 10.1093/hmg/ddu414. [PubMed: 25113746]

33. Lindsley A, Snider P, Zhou H, Rogers R, Wang J, Olaopa M, et al. Identification and characterization of a novel Schwann and outflow tract endocardial cushion lineage-restricted periostin enhancer. Dev Biol 2007;307(2):340–55 doi 10.1016/j.ydbio.2007.04.041. [PubMed: 17540359]

34. Ingram DA, Hiatt K, King AJ, Fisher L, Shivakumar R, Derstine C, et al. Hyperactivation of p21(ras) and the hematopoietic-specific Rho GTPase, Rac2, cooperate to alter the proliferation of neurofibromin-deficient mast cells in vivo and in vitro. J Exp Med 2001;194(1):57–69. [PubMed: 11435472]

35. Chen X, Zhong D, Liu D, Wang Y, Han Y, Gu J. Determination of ketotifen and its conjugated metabolite in human plasma by liquid chromatography/tandem mass spectrometry: application to a pharmacokinetic study. Rapid Commun Mass Spectrom 2003;17(22):2459–63 doi 10.1002/ rcm.1189. [PubMed: 14608613]

36. Gaudenzio N, Sibilano R, Marichal T, Starkl P, Reber LL, Cenac N, et al. Different activation signals induce distinct mast cell degranulation strategies. J Clin Invest 2016;126(10):3981–98 doi 10.1172/JCI85538. [PubMed: 27643442]

37. Theoharides TC, Alysandratos KD, Angelidou A, Delivanis DA, Sismanopoulos N, Zhang B, et al. Mast cells and inflammation. Biochim Biophys Acta 2012;1822(1):21–33 doi 10.1016/ j.bbadis.2010.12.014. [PubMed: 21185371]

38. Demetri GD, von Mehren M, Blanke CD, Van den Abbeele AD, Eisenberg B, Roberts PJ, et al. Efficacy and safety of imatinib mesylate in advanced gastrointestinal stromal tumors. N Engl J Med 2002;347(7):472–80 doi 10.1056/NEJMoa020461. [PubMed: 12181401]

39. Hensley ML, Ford JM. Imatinib treatment: specific issues related to safety, fertility, and pregnancy. Semin Hematol 2003;40(2 Suppl 2):21–5 doi 10.1053/shem.2003.50038. [PubMed: 12783371]

40. Dombi E, Ardern-Holmes SL, Babovic-Vuksanovic D, Barker FG, Connor S, Evans DG, et al. Recommendations for imaging tumor response in neurofibromatosis clinical trials. Neurology 2013;81(21 Suppl 1):S33–40 doi 10.1212/01.wnl.0000435744.57038.af. [PubMed: 24249804]

41. Plotkin SR, Blakeley JO, Dombi E, Fisher MJ, Hanemann CO, Walsh KS, et al. Achieving consensus for clinical trials: the REiNS International Collaboration. Neurology 2013;81(21 Suppl 1):S1–5 doi 10.1212/01.wnl.0000435743.49414.b6. [PubMed: 24249801]

42. Wolters PL, Martin S, Merker VL, Gardner KL, Hingtgen CM, Tonsgard JH, et al. Patient-reported outcomes in neurofibromatosis and schwannomatosis clinical trials. Neurology 2013;81(21 Suppl 1):S6–14 doi 10.1212/01.wnl.0000435747.02780.bf. [PubMed: 24249806]

43. Rodriguez-Jimenez P, Chicharro P, Munoz E, Dauden E. Long-term treatment of neurofibromatosis 1 with ketotifen. A report of three cases. Am J Med Genet A 2016;170A(4):1092–4 doi 10.1002/ajmg.a.37531. [PubMed: 26738422]

44. Dombi E, Solomon J, Gillespie AJ, Fox E, Balis FM, Patronas N, et al. NF1 plexiform neurofibroma growth rate by volumetric MRI: relationship to age and body weight. Neurology 2007;68(9):643–7 doi 10.1212/01.wnl.0000250332.89420.e6. [PubMed: 17215493]

45. Nguyen R, Dombi E, Widemann BC, Solomon J, Fuensterer C, Kluwe L, et al. Growth dynamics of plexiform neurofibromas: a retrospective cohort study of 201 patients with neurofibromatosis 1. Orphanet J Rare Dis 2012;7:75 doi 10.1186/1750-1172-7-75. [PubMed: 23035791]

46. Marichal T, Tsai M, Galli SJ. Mast cells: potential positive and negative roles in tumor biology. Cancer Immunol Res 2013;1(5):269–79 doi 10.1158/2326-6066.CIR-13-0119. [PubMed: 24777963]

47. Liao CP, Booker RC, Brosseau JP, Chen Z, Mo J, Tchegnon E, et al. Contributions of inflammation and tumor microenvironment to neurofibroma tumorigenesis. J Clin Invest 2018;128(7):2848–61 doi 10.1172/JCI99424. [PubMed: 29596064]
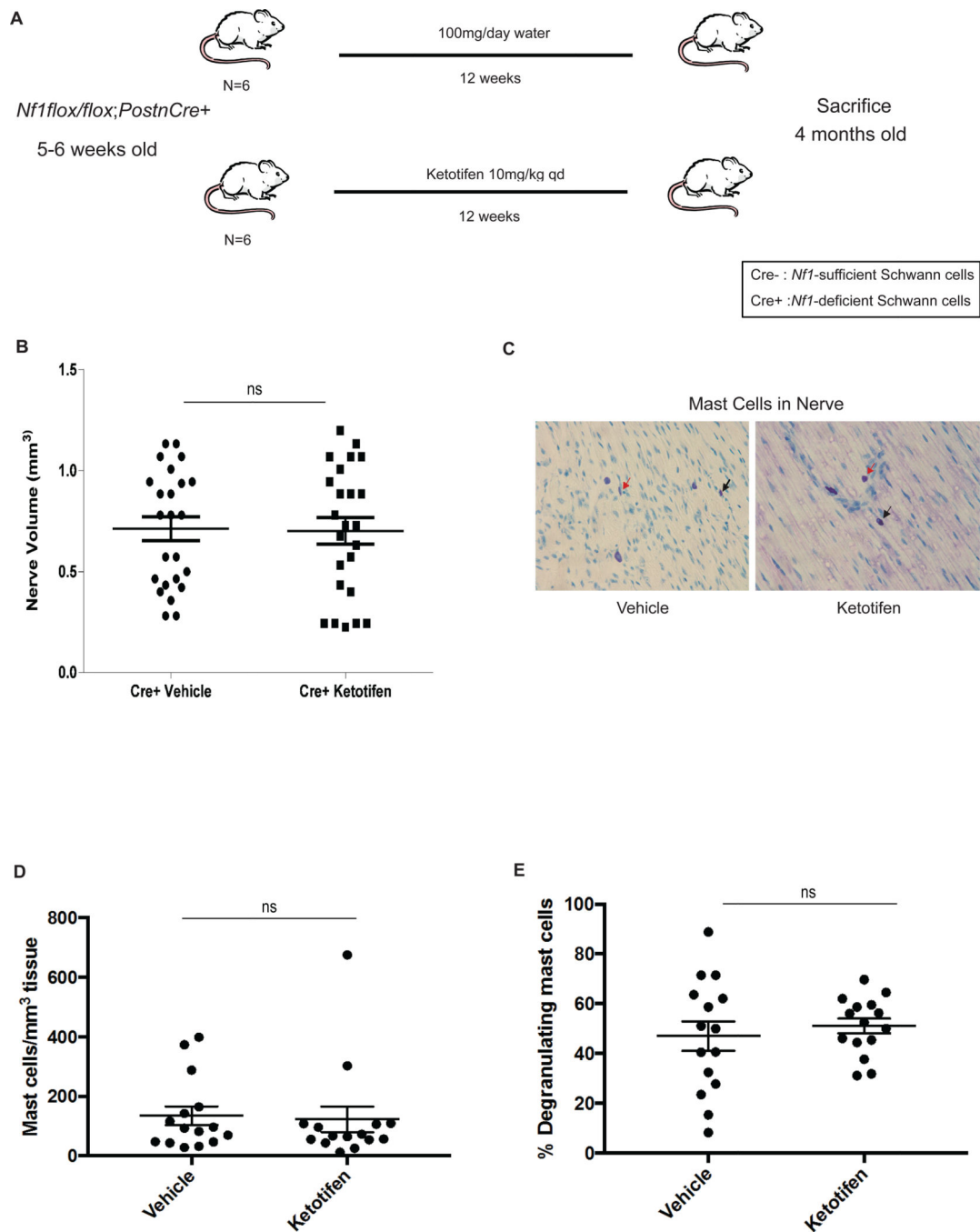
Figure 1. Ketotifen Treatment Fails to Prevent Neurofibroma Genesis in *Nf1*-deficient pups.
(**A**) Schematic of experimental design of tumor prevention study. (**B**) Proximal nerve
volume in vehicle and ketotifen-treated *Nf1^{flox/flox};PostnCre+* mice ($P = 0.9012$, ns). (**C**)
Histological analysis of toluidine blue-stained nerve tissue from water/vehicle and ketotifen-
treated *Nf1^{flox/flox};PostnCre+* mice. Images were obtained using a 40X objective lens. Black
arrows point to representative infiltrating mast cells. Red arrows point to representative
degranulating mast cells. (**D**) Quantitation of mast cell infiltration in water/vehicle- and
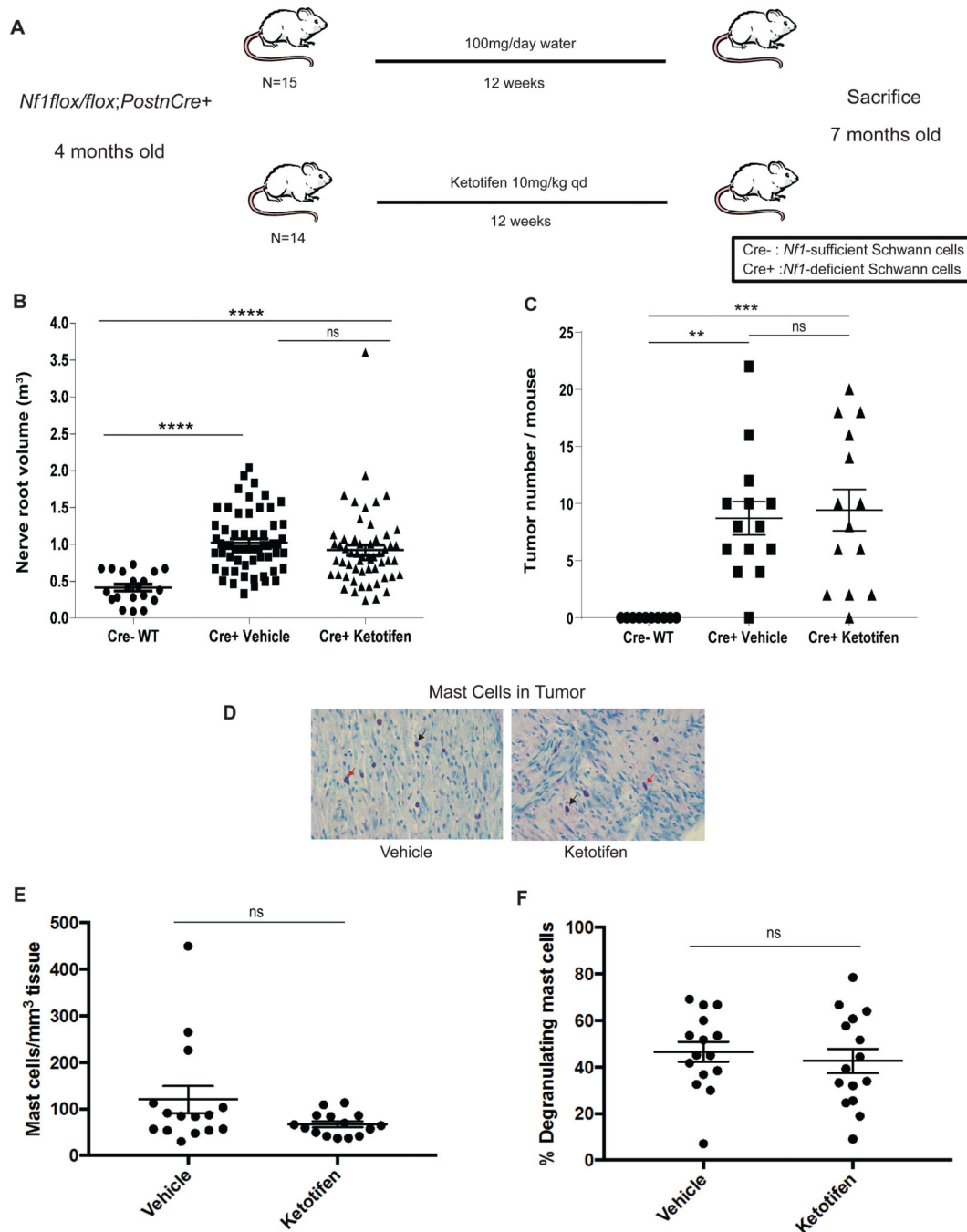ketotifen-treated *Nf1^{flox/flox};PostnCre+* mice ($P = 0.8295$, ns). (**E**) Quantitation of the

percentage of degranulating mast cells in water/vehicle- and ketotifen-treated $Nf1^{flox/flox};PostnCre+$ mice ($P = 0.5495$, ns).

Figure 2. Ketotifen Fails to Inhibit Established Neurofibroma Progression in *Nf1*-deficient Mice.
(**A**) Schematic of experimental design of established tumor regression study. (**B**) Proximal nerve root volume in water/vehicle and ketotifen-treated *Nf1flox/flox;PostnCre+* mice (*P* > 0.05, ns) and in WT *Nf1flox/flox;PostnCre-* mice (water/vehicle-treated vs WT *P* < 0.0001****; ketotifen-treated vs. WT *P* < 0.0001****). (**C**) Quantitation of tumors in water/vehicle and ketotifen-treated *Nf1flox/flox;PostnCre+* mice (*P* > 0.05, ns) and in WT *Nf1flox/flox;PostnCre-* mice (water/vehicle-treated vs WT *P* = 0.0010**; ketotifen-treated vs. WT *P* = 0.0004***). (**D**) Histological analysis of toluidine blue-stained tumor tissue from

water/vehicle- and ketotifen-treated *Nf1^flox/flox^;PostnCre+* mice. Images were obtained using a 40X objective lens. Black arrows point to representative infiltrating mast cells. Red arrows point to representative degranulating mast cells. (**E**) Quantitation of mast cell infiltration in water/vehicle- and ketotifen-treated *Nf1^flox/flox^;PostnCre+* mice ($P = 0.0821$, ns). (**F**) Quantitation of the percentage of degranulating mast cells in water/vehicle and ketotifen-treated *Nf1^flox/flox^;PostnCre+* mice ($P = 0.5686$, ns).
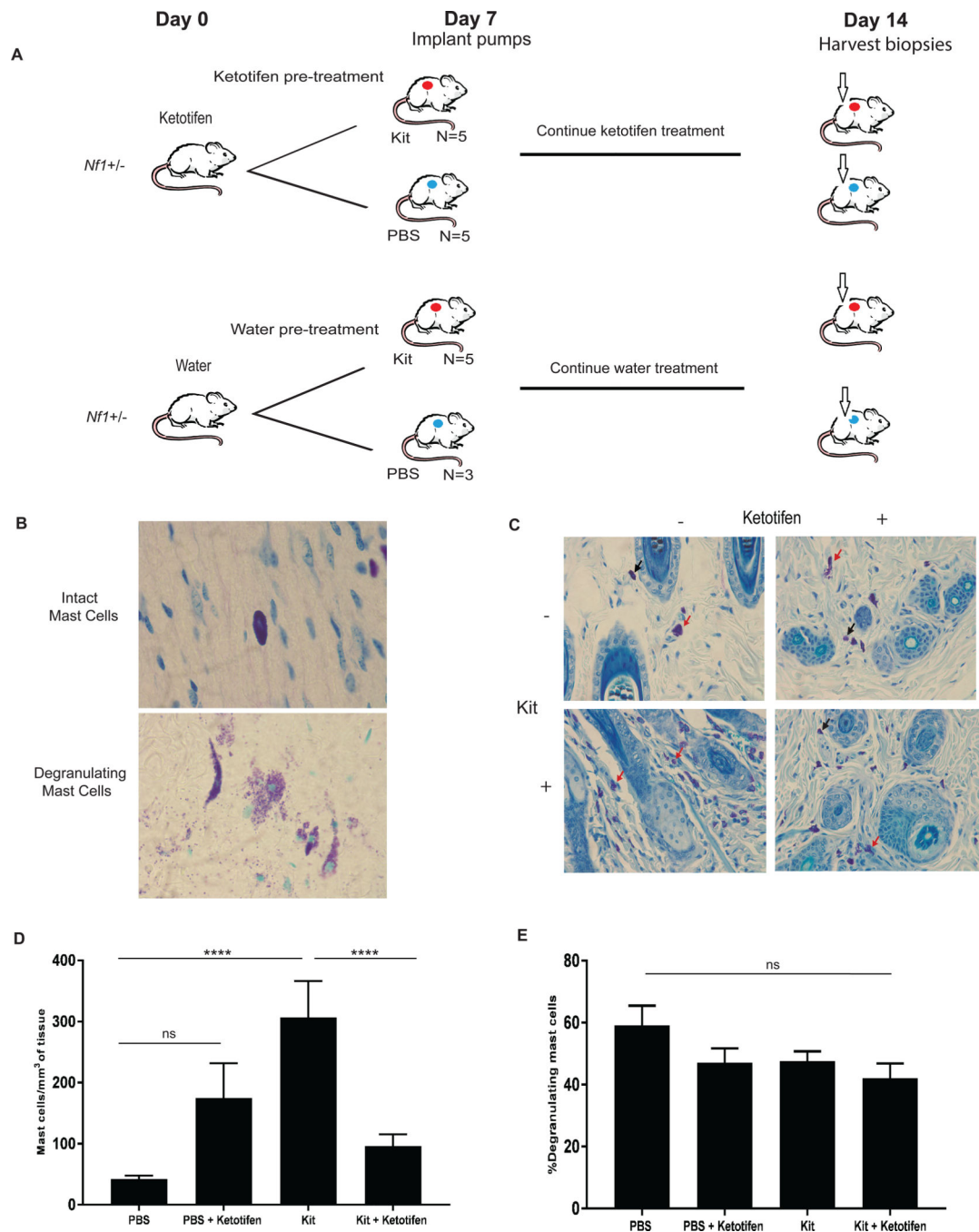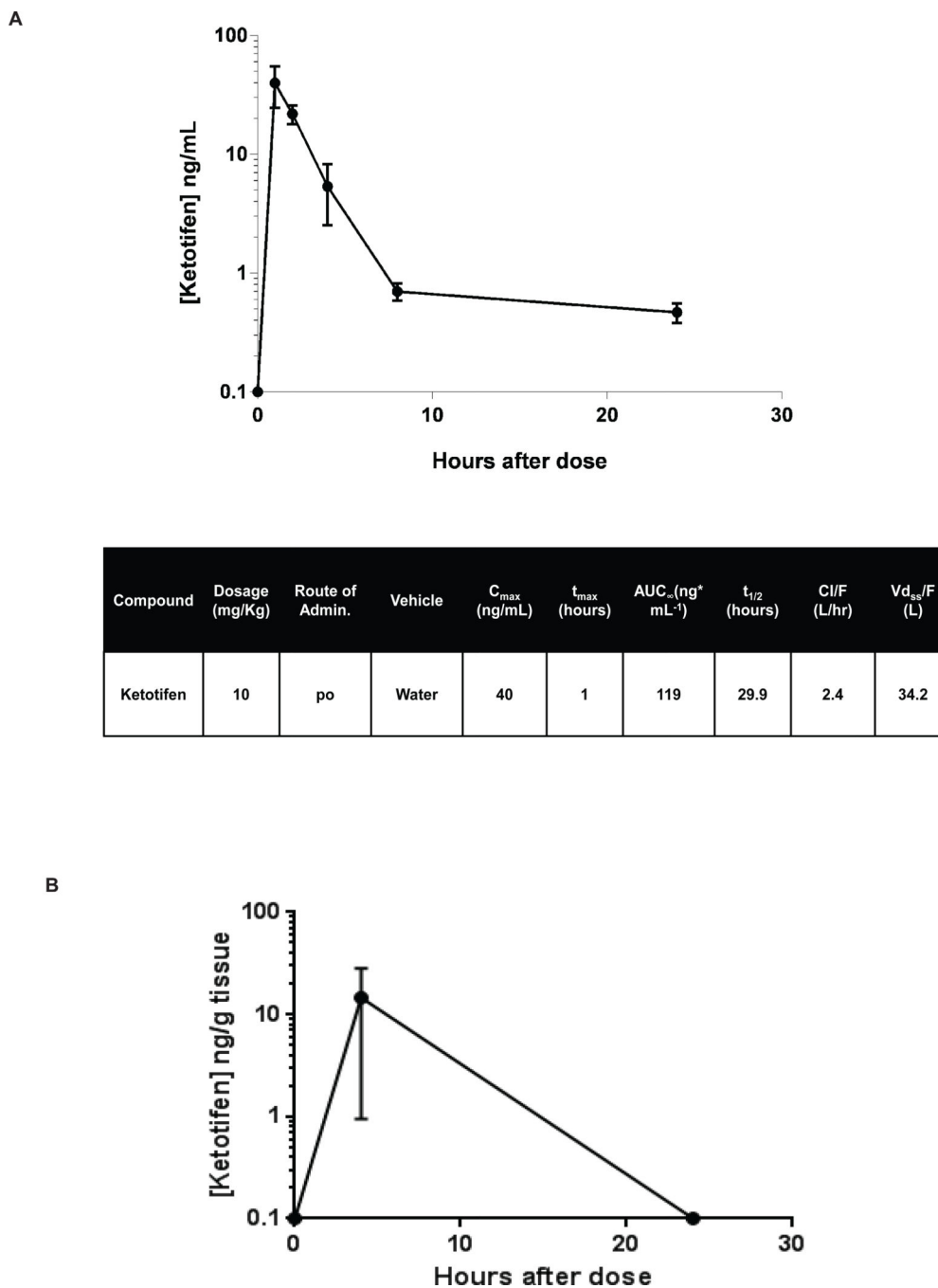
Figure 3. Effect of Ketotifen on Kit-mediated Mast Cell Infiltration and Degranulation *In Vivo*.
(**A**) Schematic of experimental design in ketotifen-pretreated/treated *Nf1*^{+/−} mice with continuous Kit ligand or PBS subcutaneous infusion. (**B**) Histological analysis demonstrating toluidine blue- stained intact versus degranulating mast cells in the skin following a 7 day Kit or PBS infusion. Image obtained using a 100X objective lens with oil. (**C**) Histological analysis of toluidine blue-stained skin biopsy of 20 μg/kg/d Kit ligand infusion-mediated and PBS infusion-mediated mast cell infiltration in ketotifen-treated and water/vehicle-treated 4-month old *Nf1*^{+/−} mice. Images were obtained using a 40X objective

lens. Black arrows point to representative infiltrating mast cells. Red arrows point to representative degranulating mast cells. (**D**) Quantification of toluidine blue-stained skin biopsy of 20 μg/kg/d Kit ligand infusion-mediated and PBS infusion-mediated mast cell infiltration per high-powered field in ketotifen-treated and water vehicle 4-month old $Nf1^{+/-}$ mice (for PBS pump vs. Kit ligand pump, $P < 0.0001****$; for PBS pump vs. ketotifen-treated PBS pump, $P > 0.05$, ns; for Kit ligand pump vs. ketotifen-treated Kit ligand pump, $P < 0.0001****$). (**E**) Quantitation of toluidine blue-stained skin biopsy of 20 μg/kg/d Kit ligand infusion-mediated and PBS infusion-mediated absolute number degranulating mast cells per high-powered field (for PBS pump vs. Kit ligand pump, $P > 0.05$, ns; for PBS pump vs. ketotifen-treated PBS pump, $P > 0.05$, ns; for Kit ligand pump vs. ketotifen-treated Kit ligand pump, $P > 0.05$, ns).

A

Compound	Dosage (mg/Kg)	Route of Admin.	Vehicle	C_{max} (ng/mL)	t_{max} (hours)	AUC_∞ (ng* mL^{-1})	$t_{1/2}$ (hours)	Cl/F (L/hr)	Vd_{ss}/F (L)
Ketotifen	10	po	Water	40	1	119	29.9	2.4	34.2

B

Figure 4. Pharmacokinetics, Safety and Tolerability of Ketotifen in *Nf1*-deficient Mice.
(**A**) HPLC-MS/MS analysis of drug concentration in the plasma of 3-month old *Nf1$^{flox/flox}$;PostnCre+* mice following a single dose of 10 mg/kg ketotifen. The plasma ketotifen concentration values over time are represented graphically. The error bars represent standard error of the mean. Key values from the pharmacokinetic data analysis are listed in in the table (n=3 mice per timepoint)(**B**). Tissue concentration was assessed at four and 24 hours in sciatic brachial and trigeminal nerve tissue (N=6).